Analysis of Urban Gas-phase Ammonia Measurements from the 2002 Atlanta Aerosol Nucleation and Real-time Characterization Experiment (ANARChE)

J.B. Nowak[1,2], L.G. Huey[3], A.G. Russell[4], D. Tian[4], J. A. Neuman[1,2], D. Orsini[3,*], S.J. Sjostedt[3], A.P. Sullivan[3], D.J. Tanner[3], R.J. Weber[3], A. Nenes[3,5], E. Edgerton[6], and F.C. Fehsenfeld[2,1]

[1]Cooperative Institute for Research in Environmental Sciences, University of Colorado, Boulder, CO 80309, USA.

[2]Chemical Sciences Division, Earth System Research Laboratory, National Oceanic and Atmospheric Administration, Boulder, CO 80305, USA.

[3]School of Earth and Atmospheric Sciences, Georgia Institute of Technology, Atlanta, GA 30332, USA.

[4]School of Civil and Environmental Engineering, Georgia Institute of Technology, Atlanta, GA 30332, USA.

[5]School of Chemical and Biomolecular Engineering, Georgia Institute of Technology, Atlanta, GA 30332, USA.

[6]Atmospheric Research and Analysis, Inc., 410 Midenhall Way, Cary, NC 27513, USA.

[*]Now at Department of Chemistry and Biochemistry, Siena College, Loudonville, NY, 12211, USA.

May 1, 2006

Revision submitted to Journal of Geophysical Research - Atmospheres

Abstract - Gas-phase ammonia (NH_3) measurements were made in July and August of 2002 during the Atlanta Aerosol Nucleation and Real-time Characterization Experiment (ANARChE) with two different Chemical Ionization Mass Spectrometry (CIMS) techniques. Correlations between the 1-min data from both instruments yielded a slope of 1.17 and an intercept of -0.295 ppbv, with a linear correlation coefficient (r^2) of 0.71. Ambient NH_3 mixing ratios ranged from 0.4 to 13 ppbv. NH_3 observations were compared to the Community Multiscale Air Quality (CMAQ) modeling system as well as a thermodynamic equilibrium model, ISORROPIA, used by CMAQ to predict NH_3 partitioning. A morning rise in both observed and modeled NH_3 mixing ratios strongly suggests a regional influence due to automobile emissions. However, at midday the predicted NH_3 decreased to less than 0.5 ppbv while the observations remained around 3 ppbv. Both observed and modeled ammonium nitrate levels were too low to support the observed midday NH_3 mixing ratios. ISORROPIA calculations of NH_3 constrained by the total measured ammonia mass (NH_3 + ammonium (NH_4^+)) agreed well with the observations (slope of 1.25 and r^2 of 0.75). For times when the net aerosol charge was near zero the agreement was excellent (slope of 1.22 and r^2 of 0.88). These results indicate that for most of the observed conditions ISORROPIA could accurately predict NH_3 partitioning. The observations suggest that local sunlight or temperature driven NH_3 sources, such as soil emissions, may be responsible for the discrepancy between the model results and measured values.

1 Introduction

Ammonia (NH_3) is an important trace gas in the troposphere. As the dominant gas-phase base NH_3 influences aerosol nucleation and composition [*Ball et al.*, 1999; *Gaydos et al.*, 2005; *Hanson and Eisele*, 2002; *McMurry et al.*, 2005; *Weber et al.*, 1998] and cloud water and precipitation pH [*Wells et al.*, 1998]. Thus, NH_3 affects regional air quality, atmospheric visibility, and acid deposition patterns [*Apsimon et al.*, 1987; *Erisman and Schaap*, 2004]. Anthropogenic emissions from livestock waste, large-scale application of fertilizer, and biomass burning are believed to be the largest atmospheric NH_3 sources [*Dentener and Crutzen*, 1994; *Schlesinger and Hartley*, 1992]. With the increased use of three-way catalytic converters, automobile emissions of NH_3 are becoming more significant in urban areas [*Fraser and Cass*, 1998; *Kean et al.*, 2000; *Moeckli et al.*, 1996; *Perrino et al.*, 2002].

This paper presents the gas-phase NH_3 observations made during the Aerosol Nucleation And Real-time Characterization Experiment (ANARChE), which took place in Atlanta, GA during August 2002. The measurements were made at the Jefferson Street Southeastern Aerosol Research and Characterization study (SEARCH) sampling site [*Hansen et al.*, 2003], an urban location, previously used for the Atlanta 1999 Supersite Experiment [*Solomon et al.*, 2003]. The aerosol size and composition instrumentation used for this study are discussed in detail elsewhere [*McMurry et al.*, 2005; *Sakurai et al.*, 2005; *Smith et al.*, 2005; *Stolzenburg et al.*, 2005]. Ancillary gas-phase measurements made at the site during the study included carbon monoxide (CO), nitrogen oxide (NO), nitric acid (HNO_3), the sum of reactive nitrogen species (NOy), ozone (O_3), sulfur dioxide (SO_2), and meteorological parameters; temperature, barometric pressure, wind direction, wind speed, and relative humidity. During ANARChE, gas-phase NH_3 was measured by two different Chemical Ionization Mass Spectrometry (CIMS)

techniques. In this paper we first describe, characterize, and compare both techniques. Ambient NH_3 levels, temporal trends, and their relationship to NH_3 sources are reported. The NH_3 observations are compared to the predictions of a regional air quality model for the month of August 2002. Lastly, we use inorganic fine particulate composition data to compare the measured partitioning of NH_3 between the gas and aerosol phases with the predictions of a thermodynamic equilibrium model. This allows us to test if the NH_3 and NH_4^+ concentrations are in equilibrium, as assumed by the regional air quality model.

2 Methods

In order to test the accuracy of newly developed NH_3 measurement capabilities, two CIMS techniques were used to detect gas-phase NH_3. Various types of chemical ionization techniques have been used to measure atmospheric trace gases [*Clemitshaw*, 2004; *de Gouw et al.*, 2004; *Fehsenfeld et al.*, 2002; *Fortner et al.*, 2004; *Huey et al.*, 2004; *Marcy et al.*, 2005; *Nowak et al.*, 2002; *Slusher et al.*, 2004]. CIMS techniques use ion-molecule reactions to selectively ionize trace species of interest in ambient air. Though both CIMS instruments in this study detected NH_3 using protonated ethanol cluster ions, the reaction conditions were different. Protonated ethanol cluster ions have been previously shown to selectively react with NH_3 under ambient atmospheric conditions with high sensitivity [*Nowak et al.*, 2002]. The National Oceanic and Atmospheric Administration – Aeronomy Laboratory, now part of the NOAA Earth System Research Laboratory's Chemical Sciences Division, (NOAA-CSD) instrument used an atmospheric pressure ionization technique while the Georgia Institute of Technology (GT) instrument used a low-pressure flow tube reactor. The instruments described below were

operated in a trailer sitting on an unpaved urban lot covered with various plant species, short grasses and weeds. The NH_3 sampling inlets, described in 2.1 and 2.2, were both approximately 2 m above ground level and 1.5 m apart. Sampling was performed from the north trailer wall over the grass/weed/soil surface.

2.1 NOAA-CSD Atmospheric Pressure Ionization

The NOAA-CSD instrument consisted of three parts: a sampling inlet, a transverse ion source, and a vacuum housing containing the ion optics, quadrupole mass spectrometer, and electron multiplier. The mass spectrometer system is essentially the same as described by *Neuman et al.* [2002]; so only the inlet and transverse ion source used for NH_3 detection will be described here.

The sampling inlet and transverse ion source are shown in Figure 1. The sampling inlet is based on that used for HNO_3 sampling described by *Neuman et al.* [2002]. All wetted inlet components, i.e. surfaces coming in contact with the ambient sample, were made from perfluoro-alkoxy (PFA) Teflon. The total inlet length was 45 cm. Ambient air was brought in through one of two ports. One port was used for measurements of ambient NH_3 while the second port was used to deliver air through a scrubber that removed NH_3 from ambient air to determine the instrumental background. A PFA rotor was actuated pneumatically to rotate and switch the ambient airflow between the two ports. As shown in Figure 1, the rotor valve was 15 cm from the ambient inlet tip, which extended 13 cm beyond the trailer wall. During ambient NH_3 measurements, ambient air was drawn through the rotor valve. When the rotor valve was actuated ambient air was drawn through a short section of PFA tubing and into a polycarbonate housing containing silicon phosphates (Perma Pure, Inc.) that formed phosphoric acid when

exposed to ambient levels of humidity and removed NH_3 from ambient air. The exit of the PFA rotor valve connected to a 25 cm long PFA tube (0.95 cm OD, 0.64 cm ID) that brought ambient air into the transverse ion source. A diaphragm pump connected to the exit of the transverse ion source through a mass flow controller pulled 4 slpm through the inlet.

The transverse ion source used here is based on that described by *Nowak et al.* [2002]. The ion source was a 9.4 cm diameter aluminum disc 2.5 cm thick with a 0.95 cm diameter hole through the center. The PFA sampling tube fit snuggly into the hole extending to the middle of the disc with an o-ring seal around the exterior of the sampling tube to prevent ambient air from leaking in. On opposite sides of the thru hole in the middle of the disc, i.e. at the end of the sampling tube, were the ^{210}Po radioactive source and the electrically isolated 100 μm pinhole. Between the radioactive source and pinhole was the ion-molecule reaction region (see Figure 1).

The protonated ethanol cluster ions were produced by flowing 1 slpm of a 900 ppmv ethanol/N_2 mixture over a foil containing ^{210}Po that releases α particles, which form $(C_2H_5OH)H^+$ through a series of reactions. These ions rapidly cluster with ethanol to form an equilibrium distribution of $(C_2H_5OH)_nH^+$, where n=1,2,3… . The $(C_2H_5OH)_nH^+$ ions were accelerated across the reaction region through the path of the ambient sample with an electric field produced by applying a potential of 1 kV to the radioactive ion source and 100 V to the pinhole. When in the reaction region, the $(C_2H_5OH)_nH^+$ ions reacted with NH_3 at atmospheric pressure

$$(C_2H_5OH)_nH^+ + NH_3 \rightarrow NH_3(C_2H_5OH)_{n-y}H^+ + y(C_2H_5OH),$$

where y is an integer less than or equal to n. A mass spectrum is shown in Figure 2. A collisional dissociation chamber (CDC) simplified the interpretation of the mass spectra obtained by gently removing weakly bounded water molecules from the protonated ethanol clusters. The

CDC also dissociated large $(C_2H_5OH)_nH^+$ cluster ions. Though the dominant $(C_2H_5OH)_nH^+$ cluster ions observed in the ambient mass spectra above were those with n = 1, 2, or 3, the distribution in the reaction region was likely dominated by larger clusters. The resulting NH_3 peaks were observed at NH_4^+, 18 atomic mass units (amu), and $(C_2H_5OH)NH_4^+$, 64 amu. This ion-molecule detection scheme is described in further detail by *Nowak et al.* [2002].

The instrument was calibrated autonomously with minimal disruption of gas flow through the calibration source or inlet. Standard addition calibrations were performed hourly with the output of an NH_3 permeation device. The permeation device was housed in a PFA temperature controlled sleeve at 40° C. 45 sccm of N_2 continuously flowed over the permeation device and through the PFA sleeve. The output from the permeation device connected to a PFA tee located at the inlet as in Figure 1. A vacuum line connected through a solenoid valve to the third leg of the tee. Calibration gas and some ambient air were removed in a 100 sccm flow through the vacuum line. This prevented the continuously flowing calibration gas from being introduced into the inlet when the solenoid was open during ambient measurements. When the solenoid valve closed the calibration gas was added to the inlet. The output of the NH_3 permeation device was periodically measured by bubbling through ultra pure water and analyzing for NH_4^+ by ion chromatography and also by UV absorption at 184.95 nm after the study [*Neuman et al.*, 2003]. The NH_3 emission rate determined by these methods over the program was 16 ± 2.5 ng/min and agreed with the manufacturer's determination by weight loss of 15 ng/min. In addition to the permeation devices, an 8.5 ppmv NH_3 in N_2 standard cylinder from Scott-Marrin, Inc. was used to calibrate the instrument every few days.

2.2 Georgia Tech Low Pressure Flow Tube Reactor

The GT CIMS instrument was composed of a sampling inlet, a low-pressure flow tube reactor, vacuum pumps, and a quadrupole mass filter with associated control electronics (Figure 3). The CIMS configuration is nearly identical to that used for peroxy acetyl nitrate (PAN) measurements described in the work of *Slusher et al.* [2004]. The two part sampling inlet is very similar to that used for HNO_3 measurements [*Huey et al.*, 2004]. Consequently, only the details relevant to the NH_3 measurements are discussed here.

The outer portion of the inlet was a 7.6 cm ID aluminum pipe that extended about 20 cm beyond the wall of the sampling trailer. A total flow of approximately 45.1 slpm was maintained in the pipe. A portion of this flow (13.6 slpm) was sampled into a custom three-way valve, constructed of PFA Teflon, which connected the center of the pipe to the CIMS sampling orifice. Most of this flow (11.6 slpm) was exhausted through a mass flow controller in series with a small diaphragm pump, with the rest (2 slpm) entering the CIMS. The valve was maintained at a constant temperature of 40°C and could be automatically switched between two flow paths. The first path was equivalent to a straight, 20 cm long, 0.65 cm ID, Teflon tube. The second configuration delivered ambient air through a phosphoric acid scrubber (Perma Pure, Inc.) to the CIMS to determine background NH_3 levels. Finally, the output of a NH_3 permeation tube (41 ng min^{-1}) was periodically delivered to the upstream end of the Teflon valve to monitor the CIMS sensitivity.

The CIMS flow reactor was operated at 20 Torr with a total flow of 7.1 slpm maintained by an oil sealed rotary vane pump. The total flow consisted of 2 slpm of ambient air and 5.1 slpm of ion source flow that consisted of primarily N_2 with approximately 1.0 % ethanol. The ethanol was delivered to the ion source by passing 100 sccm of N_2 through a room temperature trap containing liquid ethanol (ACS reagent grade). A small flow (~ 5 sccm) of dilute sulfur

hexafluoride (SF_6) in N_2 (~ 0.1 %) was also added to the ion source flow as this was found to increase signal levels by a factor of two to three.

For these conditions, the primary peaks observed in the mass spectrum were the protonated ethanol dimer and trimer ($(C_2H_5OH)_2H^+$, $(C_2H_5OH)_3H^+$). However, it is likely that larger ethanol cluster ions dominated the chemistry in the flow tube, similar to the NOAA instrument, but are not observed due to a CDC [*Nowak et al.*, 2002]. The major product ion peak observed was $(C_2H_5OH)NH_4^+$ with a smaller peak at $(C_2H_5OH)_2NH_4^+$. Masses corresponding to these major reagent and product ion peaks were measured on a four second cycle.

2.3 Instrument Performance and Comparison

Instrument performance is assessed by examining detection sensitivity, background signal, and time response. The sensitivity was determined from the response to standard addition calibrations. Standard addition calibrations of 2 to 5 ppbv were performed using the permeation devices described above every 1 to 4 hours throughout the study. The detection sensitivity for NH_3 was determined from calibrations by dividing the change in the normalized signal (the product ion signal divided by the reagent ion signal) by the standard addition NH_3 mixing ratio. This resulted in a sensitivity of normalized signal (unitless) per pptv of NH_3. This sensitivity was then interpolated between standard addition calibrations. The NH_3 concentration was calculated by dividing the normalized signal by the interpolated sensitivity. To state the sensitivity in familiar terms, such as ion counts per second (Hz) per pptv, the normalized sensitivity was multiplied by the typical reagent ion signal for each instrument.

The sensitivity for the NOAA-CSD instrument was 1 ± 0.2 Hz per pptv for 100 kHz of reagent ion, which was typical for most measurement periods. For the GT instrument the

sensitivity was typically 40 Hz per pptv for 8 MHz of reagent ion, which was typical for that system. One factor contributing to the difference in reagent ion signal between the two systems was the increased ion throughput of the octopole ion guide, used by the GT instrument, compared to the electrostatic lens stack, used by the NOAA-CSD instrument. The combined uncertainty in the accuracy of the calibration sources and sensitivity stability is estimated for the NOAA-CSD instrument at 25% and 20% for the GT system.

As described earlier both systems determined the instrumental background by scrubbing NH_3 from ambient air using silicon phosphates (Perma Pure, Inc.). Throughout the campaign, every 15 to 20 minutes ambient air was pulled through the scrubber for two to five minutes. The background of the NOAA-CSD instrument ranged between 0.1 to 1 ppbv and the difference between consecutive background measurements never exceeded 0.8 ppbv with an average difference (root mean square) between consecutive background measurements of 0.125 ppbv. For the GT instrument the background level was typically between 1.0 and 2.0 ppbv and was found to vary slowly with typical differences between consecutive backgrounds of less than 0.1 ppbv. No significant correlation was observed between background levels and observed NH_3 mixing ratios, temperature, or relative humidity, though for the GT system there was likely some dependence of background levels on ambient mixing ratios. The background in both instruments is believed to come from either the desorption of NH_3 from inlet and/or ion-molecule reactor surfaces or from NH_3 contamination either in the N_2 used as the ion source flow gas or possibly adsorbed into the liquid ethanol used for generation of ions. Since the exact source(s) of NH_3 background levels in these instruments is not well understood, it was important to perform frequent background measurements.

ANARChE NH_3 data was averaged to 1-min intervals to be consistent with archival procedures. However, both CIMS instruments collected data at higher time resolutions of 1 s, for the NOAA-CSD instrument, and 4 s, for the GT instrument. The higher time resolution data were used to determine the instrument time response. Figure 4 shows the decay of the steady-state NH_3 signals for both instruments after removal of a 2 ppbv standard addition calibration. For both instruments the signal decayed by 1/e in 10 s and $1/e^2$ within 45 s. The time response can also be well-described with a triple exponential function as used by *Ryerson et al.* [1999, 2000] to assess inlet HNO_3 transmission. The resulting equations are for the NOAA-CSD instrument

$$\% \text{ Steady-state } [NH_3] = 1 + 78*\exp(-t/2) + 16*\exp(-t/13) + 3*\exp(-t/204)$$

and for the GT instrument

$$\% \text{ Steady-state } [NH_3] = 6 + 50*\exp(-t/2) + 15*\exp(-t/12) + 26*\exp(-t/42).$$

The pre-exponential terms are expressed as a percentage of steady-state calibration level and t is the time in seconds since the calibration was terminated. This analysis suggests that 94% of the signal decay on the NOAA-CSD instrument occurred within 13 s and 91% occurred within 42 s for the GT instrument. Though the time response inferred from these methods differs, they suggest that both instruments perform independent measurements faster than the 1-min averaging time used for ANARChE data reporting. The combined uncertainty from calibration accuracy and background determination for the NOAA-CSD instrument is estimated at 25% ± 0.125 ppbv and 20% ± 0.100 ppbv for the GT instrument for a 1-min average.

Figure 5 shows the 1-min NOAA-CSD data plotted against the GT data. A weighted, bivariate regression analysis was performed on the data, where the weighting was set at $1/\sigma^2$ and σ^2 is the estimated uncertainty discussed above. The regression analysis yielded a slope of 1.17

and an intercept of -0.295 ppbv with a linear correlation coefficient (r^2) of 0.71. Though the regression analysis suggests that the NOAA-CSD data are biased high compared to the GT data, the regression line does fall within the estimated uncertainties of each instrument with an offset. The differences between the measurements were independent of ambient conditions and both observed similar diurnal trends. For simplicity the GT NH_3 data is used in the analyses presented in the rest of this work, unless otherwise noted.

2.4 Air Quality Modeling

Observations are compared to an air quality model to examine the sources of the measured NH_3 and the processes, such as aerosol partitioning, responsible for its variability. Fine particulate matter ($PM_{2.5}$) and gas-phase species modeling was performed using the US-EPA's Models-3 modeling system, including the Penn-State/NCAR Meteorological Model (MM5) [*Grell et al.*, 1999], the Carolina Environmental Program's (CEP) Sparse Matrix Operator Kernel Emissions (SMOKE) Modeling System version 1.5 [*Houyoux et al.*, 2003], and Community Multiscale Air Quality (CMAQ) version 4.3, a three-dimensional (3-D) air quality model [*Byun and Ching*, 1999]. Speciated $PM_{2.5}$ and gas phase pollutants were simulated for a one year period, (2002), using a grid of 36 km by 36 km cells covering the U.S. A sub-grid of 12 km by 12 km cells was placed over the eastern U.S., including the Atlanta area. Vertically, there were 19 layers, including an 18 m thick lowest cell, and a total column height of about 15,000 m. Meteorological fields, including temperature, relative humidity, pressure levels, three directional wind profiles etc., were generated by MM5. Emissions from each grid cell were generated by SMOKE based on the 1999 National Emission Inventory, projected to the year 2002, and subject to temporal trends (hour of day, day of week etc.) and meteorological parameters. Finally,

pollutant concentrations, in the form of hourly averages, were calculated by CMAQ. CMAQ uses ISORROPIA [*Nenes et al.*, 1998] to apportion HNO_3 and NH_3 between the gas and condensed phases, based on assuming thermodynamic equilibrium between the various inorganic species and that the particles are internally mixed.

2.5 ISORROPIA

A thermodynamic equilibrium model, ISORROPIA (http://nenes.eas.gatech.edu/ISORROPIA), was used to predict NH_3 partitioning using ANARChE observations. ISORROPIA is a computationally efficient, rigorous thermodynamic model that predicts the physical state and composition of inorganic atmospheric aerosol [*Nenes et al.*, 1998]. The $PM_{2.5}$ inorganic particle composition was measured by the GT Particle-Into-Liquid Sampler (PILS) coupled to a dual channel chromatograph [*Orsini et al.*, 2003; *Weber et al.*, 2001]. For these calculations, ISORROPIA was constrained by observations of inorganic fine particle composition, sodium (Na^+), ammonium (NH_4^+), sulfate (SO_4^{2-}), nitrate (NO_3^-), and chloride (Cl^-), total ammonia ($NH_3 + NH_4^+$), along with temperature and relative humidity data and hourly averaged HNO_3 values linearly interpolated onto the particle composition measurement time base. The model was run with a 7.5 min time-step constrained by the PILS sampling frequency. For a polluted, urban environment, such as Atlanta, the time scale for fine aerosol equilibration is expected to be similar, i.e. on the order of minutes [*Meng and Seinfeld*, 1996; *Wexler and Seinfeld*, 1991, 1992], making this a valid comparison.

3 Results and Discussion

3.1 Observations

3.1.1 NH_3 Precipitation Scavenging

The NH_3 observations made by both CIMS instruments from 19-29 August 2002 are shown in Figure 6. NH_3 mixing ratios ranged from 0.4 to 13 ppbv. The observed mixing ratios were similar to those of 0.1 to 10 ppbv reported during the Atlanta 1999 Supersite Experiment [*Baumann et al.*, 2003; *Zhang et al.*, 2003]. However, since NH_3 sources are believed to display significant variability on monthly and yearly scales, the significance of this similarity is unclear. Rather, continuous NH_3 measurements and monitoring of sources are necessary to define and interpret atmospheric NH_3 trends at a particular sampling site. The ANARChE observations showed a large amount of variability on both sub-hourly and daily time scales. This variability is much greater than the instrument uncertainties and is well captured by both instruments, as exemplified by the sharp drop in NH_3 mixing ratios observed in the afternoon of 19 August. The observed NH_3 mixing ratio in both instruments dropped from 7 ppbv to 1 ppbv over a time period of approximately 1 hour as a frontal system with precipitation passed through the area. The decrease in NH_3 mixing ratios was likely due to below cloud scavenging of NH_3 on raindrops. While it is possible that a change in air mass was responsible for the observed NH_3 decrease, there is no evidence for this in the non-soluble gas-phase pollutants such as CO. These observations are used to estimate a NH_3 below cloud scavenging coefficient.

Below cloud scavenging of NH_3 depends on many factors such as rain droplet size distribution, rainfall intensity, droplet pH, cloud base height, and temperature [*Asman*, 1995; *Kumar*, 1985, 1986; *Mizak et al.*, 2005; *Shimshock and DePena*, 1989]. Unfortunately, of these parameters only temperature was measured during the ANARChE study. Model calculations show that the time required for a highly soluble gas, like NH_3, to reach equilibrium is much

longer than the time needed for a typical raindrop to fall from the cloud base to ground level [*Kumar*, 1985; *Shimshock and DePena*, 1989]. Therefore, a simple equilibrium calculation is not appropriate here. During rainfall, the gas-phase NH_3 concentration decreases with time according to the first order scavenging coefficient (Λ) assuming an uniform initial concentration and is described by the following equation [*Kumar*, 1985]

$$[NH_3](t) = [NH_3]^o \exp^{(-\Lambda t)} \quad (1)$$

Using the ANARChE NH_3 observations and assuming the changes in NH_3 were caused entirely by rainfall, t = 60 min, $[NH_3]^o$ = 7 ppbv, and $[NH_3]$ (t) = 1 ppbv, Λ is calculated to be 3.24×10^{-2} min^{-1}. This scavenging coefficient is similar to previous observations [*Shimshock and DePena*, 1989; *Mizak et al,* 2005] and model calculations [*Kumar*, 1985; *Asman,* 1995]. Though not enough rainfall parameters were measured during ANARChE to allow for a rigorous comparison to previous results, the scavenging rate calculated during ANARChE is comparable with previous work and explains why concentrations of a soluble gas like NH_3 did not go to zero during the storm with two caveats. First, there is no spatial data available from ANARChE supporting the initial premise that NH_3 is uniformly distributed in the planetary boundary layer (PBL). Second, no emission term is included in the derivation of equation (1). For example, in an urban area automobile emissions, believed to be a source of NH_3, could increase during a rainstorm due to increases in automobile usage and traffic congestion. Thus, it is possible that for the ANARChE observations, Λ is greater than calculated from the observations by equation (1) with NH_3 emissions buffering the observed mixing ratios.

The rapid variability in NH_3 highlights the utility of high time resolution instruments even at ground sites. Measurements on this time scale showed that the NH_3 mixing ratio varied significantly and more rapidly than could be discerned from most passive filter-type monitoring

techniques. High time resolution measurements are important to atmospheric process studies, such as precipitation scavenging and the analysis by *McMurry et al.* [2005] suggesting that the sensitivity of particle production during ANARChE to NH_3 concentrations was much higher than predicted by ternary nucleation theory [*Napari et al.*, 2002].

3.1.2 NH_3 Source Identification

Longer time-scale changes in NH_3 mixing ratios are investigated with respect to meteorology and emission sources. Throughout the study, winds were light (average wind speed of 1.3 m s^{-1}) and variable. No correlation was observed between NH_3 and either wind direction or speed, indicating no significant transport of NH_3 from a local point source. Except for the scavenging event described above, NH_3 also showed no correlation with relative humidity or temperature. A general diurnal trend was consistently observed with NH_3 mixing ratios increasing in the morning, consistent with the morning rush hour, and remaining elevated during the day before decreasing at night. Thus, the observed trend was somewhat consistent with urban traffic patterns and automobiles as an urban NH_3 source.

The connection between this daytime increase and automobile emissions was further examined using the ancillary gas-phase data. The GT NH_3, CO, and NOy data were binned into hourly averages (solid line) and medians (bars) according to time of day (Figure 7) in Eastern Standard Time (EST) with the horizontal bars representing the 25^{th} and 75^{th} percentile of the data. Though a diurnal trend was observed on many individual days, when plotted as hourly medians, the day to day variability in NH_3 mixing ratios largely obscures this trend and causes the large range between the 25^{th} and 75^{th} percentiles. Even so, there is a daytime increase in both the median and average hourly values with small peaks between 7 and 8 am and 4 and 5 pm.

The CO and NOy trends were similar to each other, but different than the observed NH_3 trend. The CO and NOy mixing ratios were higher at night instead of during the day and peaked between 6 and 7 am. It is likely that the morning peaks seen in CO and NOy were due to morning rush hour automobile emissions along with a low mixing depth. Little correlation was observed between NH_3 and CO, NOy, NO, or NO/CO ratio. There is little evidence in the available gas-phase data for strong NH_3 point sources influencing the site. Given the meteorology (light and variable winds) and location (Midtown, Atlanta), the NH_3 source is likely a large, diffuse, area source or multiple point sources surrounding the site rather than a single point source, such as an industrial facility.

Trends of NH_3, CO, and NOy were also influenced by the PBL height. For a long-lived species, like CO, one explanation for the increase in nighttime mixing ratios is emissions into a shallow nocturnal boundary layer with the decrease in mixing ratios as the sun rises due to surface heating and the break-up of this layer. Conversely, for a species like NH_3 that is lost to surfaces, the shallow nocturnal boundary layer could increase the surface loss rate. Combined with a decrease in urban sources, such as reduced automobile traffic at night, this would result in a decrease of nighttime mixing ratios. Again, as the sun rises and the Earth's surface heats, this shallow boundary layer breaks up and the surface loss rate decreases along with an increase in urban automobile emissions as morning rush hour begins.

Relatively elevated NH_3 levels during the day, and lack of a large decrease at midday as observed for CO and NOy, suggest that the source(s) of NH_3 impacting the site differ from the major sources of CO (gasoline fueled vehicles) and NOy (diesel and gasoline engines). While the morning increases are similar, and may be explained by NH_3 emissions from catalytically-controlled automobiles (e.g., [*Fraser and Cass*, 1998; *Kean et al.*, 2000; *Moeckli et al.*, 1996;

Perrino et al., 2002]), the continued relatively high levels during the bulk of the day suggest that the source(s) of NH_3 increase in strength as the mixing depth increases (e.g., is temperature or sunlight driven) or that there is a relatively high level of NH_3 in the PBL being entrained downwards. Though we are unable to identify all NH_3 sources or the cause for the observed daily NH_3 trend, both CIMS instruments deployed during ANARChE observed similar variability in ambient NH_3 mixing ratios. Comparisons with a regional air quality model are performed to further investigate NH_3 sources and sinks.

3.2 Model and Measurement Comparison

3.2.1 CMAQ Comparison

Observed NH_3 levels and the resulting diurnal variation were compared to those predicted by CMAQ. The short-time scale variability seen in the observations is not captured in the model results. This disagreement is expected because of the relatively large grid size of the model compared to the point measurement, and the coarse temporal resolution of the emission and meteorology inputs to CMAQ. The daily average NH_3 mixing ratio predicted by the model (1.5 ppbv) does agree within a factor of 2 with the observations (2.9 ppbv). However, the daily trend predicted by the model is very different than that observed. The GT NH_3 observations (top panel) and model predicted values (bottom panel) were binned into hourly averages and medians according to time of day in Figure 8. The NH_3 trend from the regional air quality model is similar to that of CO and NOy (Figure 7). All three peak between 6 and 7 am, consistent with automobile emissions. As discussed earlier, the observed NH_3 levels also increased in the morning though later than CO and NOy. The most striking difference between the NH_3 observation and model trends is the midday behavior. The model NH_3 values on average

decrease to below 0.5 ppbv at midday as the planetary boundary layer increases in height and becomes well mixed, following the behavior observed for CO and NOy. Contrary to the model, the NH_3 observations remain relatively constant at 3 ppbv throughout the day.

Model prediction of ammonium nitrate levels and the release of NH_3 from ammonium nitrate volatilization are examined as a possible cause for the difference with the observations. NH_4^+ and NO_3^- observations were binned into hourly averages and compared to the model results (Figures 9 and 10). The NH_4^+ observations show no diurnal trend with little change in concentration or variability throughout the day. Unlike the observations a diurnal trend is seen in the model results with modeled NH_4^+ level peaking between 7 am and 8 am, similar to CO and NOy observations. Though the model predicts average NH_4^+ levels higher than observed both the observations and model results are within each other's variability. In the case of NO_3^-, the model results are in good agreement with the observations (Figure 10). A similar diurnal trend is seen in both with NO_3^- levels peaking between 6 and 8 am then dropping to near zero at midday presumably due to ammonium nitrate volatilization. Average modeled NO_3^- levels are approximately 50% higher than measured but as with NH_4^+ they each are within the variability of the other. On average, if all the NO_3^-, either modeled or observed, were ammonium nitrate aerosol, then complete volatilization would release the equivalent of less then 1 ppbv of NH_3. This is significantly less than the 3 ppbv of NH_3 observed on average at midday during the study. Because of the agreement between observed and modeled NO_3^- levels and the low levels of NO_3^-, the difference in midday NH_3 levels is not due to model under prediction of ammonium nitrate levels.

A major NH_3 sink is scavenging by aerosol SO_4^{2-}. SO_4^{2-} observations were binned into hourly averages and compared to the model results (Figure 11). On average, the model agrees

well with the observations, typically within 20% and always within a factor of two. Given the good agreement between model SO_4^{2-} and the observations, it seems unlikely that the NH_3 gas-phase discrepancy is due only to an overestimation of NH_3 scavenging.

The difference in midday behavior between the observations and the model could be due to small-scale inhomogeneities in sources not captured in the regional air quality model. One example of an inhomogeneous small-scale source is soil emissions. NH_3 soil emissions are believed to be a function of soil temperature, pH, and nitrogen content [*Roelle and Aneja*, 2005]. The short time-scale variability in the NH_3 observations that was greater during the day than at night provides some evidence that the ANARChE NH_3 observations were influenced by soil emission or other biological activity at the ground surface. Since both inlets sample over a soil/plant surface, one possible explanation for the observed short time-scale variability is fluctuations in the emission of NH_3 from the surface either from soil, plants, or other surface biological activity and/or changes in turbulent mixing upward from surface as temperature and sunlight change during the day. These small-scale atmospheric inhomogeneities may be responsible for some of the short-time scale variations observed between the two instruments.

The impact of small-scale local sources, such as soil emissions, on ambient NH_3 mixing ratios likely decreases rapidly as a function of distance from the source. All ANARChE sampling was performed at 2 m, so no information on the vertical distribution of NH_3 at the site is available. Any comparison between a measurement at a fixed height site and the grid cell average from a regional model would likely reveal a disagreement for compounds with potentially large sources and sinks at the ground. Small-scale local sources like these may not have the same impact on regional air quality as an industrial facility or major highway, however, they could still affect ground level nucleation, i.e. neighborhood scale air quality, and are

important for nitrogen cycling. Regardless of how local small-scale sources may affect the observation/model comparison, the morning rise in NH_3 mixing ratios observed in both strongly suggests a regional influence due to automobile emissions.

3.2.2 ISORROPIA Comparison

Another possible explanation for the daytime discrepancy between the observed and modeled NH_3 trends is that the gas and aerosol phases are not in thermodynamic equilibrium. The thermodynamic equilibrium between gas and aerosol NH_3 is a complex function of aerosol pH, the relative amounts of aerosol species (SO_4^{2-}, NO_3^-, and Cl^-), the gas-phase level of hydrochloric acid (HCl) and HNO_3, as well as the ambient temperature and relative humidity (which affect the equilibrium constants, aerosol deliquescence, and amount of water uptake) [e.g., *Nenes et al.*, 1998; *Meng and Seinfeld*, 1996; *Wexler and Seinfeld*, 1991, 1992; *Zhang et al.*, 2002]. To examine this possibility the ISORROPIA thermodynamic equilibrium model [*Nenes et al.*, 1998], as used in the CMAQ air quality model, was used to predict NH_3 partitioning based on measurements. Due to limited data coverage only data collected from 15-31 August 2002 were used as an input for ISORROPIA. In Figure 12, the predicted NH_3 is plotted against the measured NH_3. There is good agreement between the model results and observations with an unweighted linear regression analysis yielding a slope of 1.25, within the combined uncertainties of the model input data, with an intercept of 0.012 $\mu g\ m^{-3}$ and an r^2 of 0.75. The agreement within the uncertainties suggests that the assumption of thermodynamic equilibrium on the 7.5 min time scale is appropriate for most of the ANARChE data examined here.

The data in Figure 12 are colored by the net charge in μEq m^{-3} determined from the PILS observations of NH_4^+, Na^+, NO_3^-, SO_4^{2-}, and Cl^- used as inputs in ISORROPIA. The net charge was calculated by converting the PILS data from μg m^{-3} to μEq m^{-3} and then taking the difference between the sum of the cations (NH_4^+, Na^+) and the sum of the anions (NO_3^-, SO_4^{2-}, Cl^-). Two distinct populations of data are outliers in Figure 12. The net charge in each of these populations indicates that the inorganic component of the aerosol in each is far from neutralized. For the very acidic cases, where there is free sulfuric acid in the aerosol, (substantial amounts of H^+ results in a negative net charge, red) ISORROPIA underpredicts the NH_3 concentrations. ISORROPIA assumes (for computational efficiency) the first dissociation of H_2SO_4 to be complete resulting in a higher concentration of aqueous H^+, which tends to bias the NH_3 concentrations low. While for the most basic (positive net charge in purple) data the model over predicts NH_3 concentrations; this can be from the presence of organic anions (which can partially neutralize NH_3) and are not considered by the model (as in most others). Excluding these data from the linear regression analysis has little affect on the slope, 1.22 compare to 1.25, with an r^2 of 0.88, further emphasizing the excellent agreement between the observed and predicted ammonia partitioning and indicating the aerosol was suitable for modeling by ISORROPIA (i.e., typically partially neutralized sulfates and bisulfates with negligible soluble organic electrolytes).

A similar analysis was performed by *Zhang et al.* [2002], using data from the 1999 Atlanta Supersite study. In their analysis, the measured and calculated NH_3 concentrations differed by orders of magnitude suggesting that thermodynamic equilibrium does not apply. However, *Zhang et al.* [2002] also found that the predicated NH_3 was extremely sensitive to the aerosol acidity. Adjusting aerosol acidity, in their case by reducing SO_4^{2-} concentrations by ~15%, brought the predicted NH_3 concentrations into good agreement with NH_3 observations.

This lead to speculation that species not measured by the PILS, such as organics, contributed to aerosol acidity, or that the PILS systematically over measured SO_4^{2-} (see *Weber et al*., [2003] for SO_4^{2-} measurement intercomparisons), and that the assumed thermodynamic equilibrium was applicable though not included in ISORROPIA. For the majority of data collected during ANARChE there is excellent agreement between ISORROPIA NH_3 predictions and observations. However, similar to the results by *Zhang et al.* [2002], the largest discrepancies between the model and observations appear to be coupled to aerosol pH. This could indicate that these time periods were not in thermodynamic equilibrium or that the conditions were not applicable to ISORROPIA.

The good agreement between ISORROPIA-predicted NH_3 concentrations and those observed suggests that the discrepancy between the air quality model predictions and the observations is not due to the partitioning of NH_3 between the aerosol and gas-phases. Rather, the discrepancy is likely due to missing NH_3 sources in the air quality model, either large, regional sources or local small-scale sources whose effect is confined to ground level and have minimal regional impact. A major and ubiquitous modeled source would cause significantly higher levels of NH_3, NH_4^+, and NO_3^- at other times and throughout the domain, leading to higher levels of those species regionally as compared to observations. Since ANARChE NH_3 observations (Figure 8) disagree with the model primarily at midday, it is more likely that local sources are the responsible for the majority of midday NH_3, though ammonium nitrate volatilization also contributes.

4 Conclusions

Gas-phase NH_3 was measured by two different CIMS techniques during the ANARChE study in Atlanta in August 2002. The sensitivities for the instruments, as determined by standard addition calibrations, were 1 ± 0.2 Hz per pptv for 100 kHz of reagent ion for the NOAA-CSD instruments and typically 40 Hz per pptv for 8 MHz of reagent ion for the GT instrument. Analysis of the signal decay after calibration suggested that the time response of both instruments was less than 1 minute. The instrument background, determined by scrubbing NH_3 from ambient air, ranged from 0.1 ppbv to 1 ppbv for the NOAA-CSD instrument and 1 ppbv to 2 ppbv for the GT instrument. The precision of each instrument, defined here as the average difference between consecutive backgrounds, was 0.125 ppbv and 0.1 ppbv, respectively. The combined uncertainty for the 1 min. data was estimated at 25% ± 0.125 ppbv for the NOAA-CSD instrument and 20% ± 0.100 ppbv for the GT instrument. A weighted, regression analysis of the correlation between the two measurements yielded a slope of 1.17 and an intercept of -0.295 ppbv with an r^2 of 0.71. The measurement differences showed no biases dependent on ambient conditions.

The results presented here show no clear advantage to either of the CIMS techniques used during ANARChE (atmospheric pressure ionization vs. low-pressure flow tube reactor). The NOAA atmospheric pressure ionization technique displayed a faster time response with a lower but more variable background. Though the time response of the GT low-pressure flow tube reactor was slower, it had greater total signal and in turn higher sensitivity, albeit with a slightly higher but more stable background. The time response of both instruments (< 1 min) was adequate for the goals of this study and of many ground-based programs. However, improvements need to be made to both sampling schemes to make measurements at the pptv

level in 1s from mobile platforms, such as aircraft, where the high sensitivity of the CIMS instruments can be utilized in expected low NH_3 environments like the free troposphere.

The area in need of most improvement is understanding and controlling the instrumental background. In the case of the NOAA-CSD instrument, with a sensitivity of 1 Hz/pptv, the noise imposed by counting statistics on the instrumental background is equivalent to 32 pptv. For the GT instrument, with a sensitivity of 40 Hz/pptv the noise imposed by counting statistics is equivalent to 5 pptv. While this precision was not a limitation during ANARChE where ambient mixing ratios were always greater than 2 ppbv, measurements of ambient levels in the 10 to 100 pptv range will require the background to be reduced. To improve either instrument, both the absolute level and the variability in the instrumental background need to be reduced.

Observed NH_3 mixing ratios ranged from 0.4 to 13 ppbv and showed a large amount of variability on both sub-hourly and daily time scales. No correlation was observed between NH_3 and either wind direction or speed indicating no significant transport of NH_3 from a local point source. A general, diurnal trend consistent with urban automobile traffic was observed with NH_3 mixing ratios increasing in the morning and remaining elevated during the day before decreasing at night. However, no correlation was observed between NH_3 and the ancillary data indicative of fresh automobile emissions, such as CO, NOy, NO or NO/CO ratio. NH_3 observations were compared to those predicted by CMAQ. Comparison of the observed and predicted NH_3 diurnal trend revealed that both increase in the morning, though the observations later than the predictions. This agreement suggests that the morning rise in NH_3 mixing ratios is due to the Atlanta morning rush hour along with a reduced mixing height. However, average values differed at midday with the model values decreasing to less than 0.5 ppbv while the observations remained steady at 3 ppbv. Given the good agreement between model SO_4^{2-} and the

observations, it seems unlikely that the NH_3 gas-phase discrepancy was due only to an overestimation of NH_3 scavenging. The ISORROPIA thermodynamic equilibrium model was used to examine the validity of the assumption of equilibrium of NH_3 between the aerosol and gas-phase during ANARChE. Though ISORROPIA, constrained by the total observed ammonia ($NH_3 + NH_4^+$), over predicted the observed NH_3 levels, the agreement (slope of 1.25 and r^2 of 0.75) indicates that the assumption of thermodynamic equilibrium was reasonable. This result suggests that the discrepancy between the regional model and observations is more likely due to missing NH_3 sources in the model than non-equilibrium conditions or overestimation of sinks. In light of the agreement between the observed and modeled ammonium and nitrate, it is likely that the missing sources are local.

Acknowledgements: The author, John B. Nowak, was supported by a National Research Council Research Associateship Award at the NOAA Aeronomy Laboratory during the ANARChE study. L. Gregory Huey was supported by NOAA OGP# NA04OAR4310088. Rodney J. Weber gratefully acknowledges support for the aerosol composition measurements by the Department of Energy contract DE-FG02-98R62556 through a subcontract with the University of Minnesota (Peter McMurry) under contract T5306498002. We also appreciate the support of Peter McMurry in organizing the ANARChE study and John Jansen (The Southern Company) in providing site access and sampling laboratories.

References

Apsimon, H. M., et al. (1987), Ammonia emissions and their role in acid deposition, *Atmos. Environ.*, *21*, 1939-1946

Asman, W. A. H. (1995), Parameterization of below-cloud scavenging of highly soluble gases under convective conditions, *Atmos. Environ.*, *29*, 1359-1368.

Ball, S. M., D. R. Hanson, F. L. Eisele, and P. H. McMurry (1999), Laboratory studies of particle nucleation: Initial results for H_2SO_4, H_2O, and NH_3 vapors, *J. Geophys. Res.*, *104*(D19), 23709-23718.

Baumann, K., F. Ift, J. Z. Zhao, and W. L. Chameides (2003), Discrete measurements of reactive gases and fine particle mass and composition during the 1999 Atlanta Supersite Experiment, *J. Geophys. Res.*, *108*(D7), 8416, doi:10.1029/2001JD001210.

Byun, D. W., and J. K. S. Ching (1999), Sciene algorithms of the EPA-Models-3 Community Multiscale Air Quality (CMAQ) Modeling System, Office of Research and Development, Washington, DC 20460, EPA/600/R-99/030.

Clemitshaw, K. C. (2004), A review of instrumentation and measurement techniques for ground-based and airborne field studies of gas-phase tropospheric chemistry, *Critical Reviews In Environmental Science And Technology*, *34*, 1-108.

de Gouw, J., C. Warneke, R. Holzinger, T. Klupfel, and J. Williams. (2004), Inter-comparison between airborne measurements of methanol, acetonitrile and acetone using two differently configured PTR-MS instruments, *International Journal Of Mass Spectrometry*, *239*, 129-137, doi:10.1016/j.ijms.2004.07.025.

Dentener, F. J., and P. J. Crutzen (1994), A 3-dimensional model of the global ammonia cycle, *J. Atmos. Chem.*, *19*, 331-369.

Erisman, J. W., and M. Schaap (2004), The need for ammonia abatement with respect to secondary PM reductions in Europe, *Environ. Pollut.*, *129*, 159-163.

Fehsenfeld, F. C., L. G. Huey, E. Leibrock, R. Dissly, E. Williams, T. B. Ryerson, R. Norton, D. T. Sueper, and B. Hartsell (2002), Results from an informal intercomparison of ammonia measurement techniques, *J. Geophys. Res.*, *107*(D24), 4812, doi:10.1029/2001JD001327.

Fortner, E. C., J. Zhao, and R. Zhang (2004), Development of ion drift-chemical ionization mass spectrometry, *Anal. Chem.*, *76*, 5436-5440, doi:10.1021/ac0493222.

Fraser, M. P., and G. R. Cass (1998), Detection of excess ammonia emissions from in-use vehicles and the implications for fine particle control, *Environ. Sci. Technol.*, *32*, 1053-1057.

Gaydos, T. M., C. O. Stanier, and S. N. Pandis (2005), Modeling of in situ ultrafine atmospheric particle formation in the eastern United States, *J. Geophys. Res.*, *110*, D07S12, doi:10.1029/2004JD004683.

Grell, G. A., et al. (1999), A description of the fifth generation Penn State/NCAR mesoscale model (MM5), NCAR Technical Note, NCAR/TN-398+STR, edited.

Hansen, D. A., E. S. Edgerton, B. E. Hartsell, J. J. Jansen, N. Kandasamy, G. M. Hidy, and C. L. Blanchard (2003), The southeastern aerosol research and characterization study: Part 1-overview, *J. Air & Waste Manage. Assoc.*, *53*, 1460-1471.

Hanson, D. R., and F. L. Eisele (2002), Measurement of prenucleation molecular clusters in the NH_3, H_2SO_4, H_2O system, *J. Geophys. Res.*, *107*(D12), 4158, doi:10.1029/2001JD001100.

Houyoux, M., et al. (2003), *Sparse Matrix Operator Kernel Emissions Modeling system (SMOKE): User Manual, Version 2.0*, Carolina Environmental Program.

Huey, L. G., et al. (2004), CIMS measurements of HNO_3 and SO_2 at the South Pole during ISCAT 2000, *Atmos. Environ, 38*, 5411-5421, doi:10.1016/j.atmosenv.2004.04.037.

Kean, A. J., R. A. Harley, D. Littlejohn, and G. R. Kendall (2000), On-road measurement of ammonia and other motor vehicle exhaust emissions, *Enviro. Sci. Technol.*, *34*, 3535-3539.

Kumar, S. (1985), An eulerian model for scavenging of pollutants by raindrops, *Atmos. Environ.*, *19*, 769-778.

Kumar, S. (1986), Reactive scavenging of pollutants by rain - a modeling approach, *Atmos. Environ.*, *20*, 1015-1024.

Marcy, T. P., R.S. Gao, M.J. Northway, P.J. Popp, H. Stark, and D.W. Fahey (2005), Using chemical ionization mass spectrometry for detection of HNO_3, HOl, and $ClONO_2$ in the atmosphere, *International Journal Of Mass Spectrometry*, *243*, 63-70, doi:10.1016/j.ijms.2004.11.012.

McMurry, P. H., et al. (2005), A criterion for new particle formation in the sulfur-rich Atlanta atmosphere, *J. Geophys. Res.*, *110*, D22S02, doi:10.1029/2005JD005901.

Meng, Z. Y., and J. H. Seinfeld (1996), Time scales to achieve atmospheric gas-aerosol equilibrium for volatile species, *Atmos. Environ.*, *30*, 2889-2900.

Mizak, C. A., S. W. Campbell, M. E. Luther, R. P. Carnahan, R. J. Murphy, and N. D. Poor (2005), Below-cloud ammonia scavenging in convective thunderstorms at a coastal research site in Tampa, FL, USA, *Atmos. Environ.*, *39*, 1575-1584, doi:10.1016/j.atmosenv.2004.10.008.

Moeckli, M. A., M. Fierz, and M. W. Sigrist (1996), Emission factors for ethene and ammonia from a tunnel study with a photoacoustic trace gas detection system, *Environ. Sci. Technol.*, *30*, 2864-2867.

Napari, I., M. Noppel, H. Vehkamäki, and M. Kulmala (2002), Parametrization of ternary nucleation rates for H_2SO_4-NH_3-H_2O vapors, *J. Geophys. Res.*, *107*(D19), 4381, doi:10.1029/2002JD002132.

Nenes, A., S. N. Pandis, and C. Pilinis (1998), ISORROPIA: A new thermodynamic equilibrium model for multiphase multicomponent inorganic aerosols, *Aquat. Geochem.*, *4*, 123-152.

Neuman, J. A., et al. (2002), Fast-response airborne in situ measurements of HNO_3 during the Texas 2000 Air Quality Study, *J. Geophys. Res., 107*(D20), 4436, doi:10.1029/2001JD001437.

Neuman, J. A., T. B. Ryerson, L. G. Huey, R. Jakoubek, J. B. Nowak, C. Simons, and F. C. Fehsenfeld (2003), Calibration and evaluation of nitric acid and ammonia permeation tubes by UV optical absorption, *Environ. Sci. Technol.*, *37*, 2975-2981.

Nowak, J. B., L. G. Huey, F. L. Eisele, D. J. Tanner, R. L. Mauldin III, C. Cantrell, E. Kosciuch, and D. D. Davis (2002), Chemical ionization mass spectrometry technique for detection of dimethylsulfoxide and ammonia, *J. Geophys. Res.*, *107*(D18), 4363, doi:10.1029/2001JD001058.

Orsini, D. A., Y. Ma, A. Sullivan, B. Sierau, K. Baumann and R. J. Weber (2003), Refinements to the particle-into-liquid sampler (PILS) for ground and airborne measurements of water soluble aerosol composition, *Atmos. Environ.*, *37*, 1243-1259, doi:10.1016/S1352-2310(02)01015-4.

Perrino, C., M. Catrambone, A. Di Menno Di Bucchianico, and I. Allegrini (2002), Gaseous ammonia in the urban area of Rome, Italy and its relationship with traffic emissions, *Atmos. Environ.*, *36*, 5385-5394.

Roelle, P. A., and V. P. Aneja (2005), Modeling of ammonia emissions from soils, *Environ. Eng. Sci.*, *22*, 58-72.

Ryerson, T. B., L. G. Huey, K. Knapp, J. A. Neuman, D. D. Parrish, D. T. Sueper, and F. C. Fehsenfeld (1999), Design and initial characterization of an inlet for gas-phase NO_y measurements from aircraft, *J. Geophys. Res.*, *104*(D5), 5483–5492.

Ryerson, T. B., E. J. Williams, and F. C. Fehsenfeld (2000), An efficient photolysis system for fast-response NO_2 measurements, *J. Geophys. Res.*, *105*(D21), 26,447–26,462.

Sakurai, H., M. A. Fink, P. H. McMurry, L. Mauldin, K. F. Moore, J. N. Smith, and F. L. Eisele (2005), Hygroscopicity and volatility of 4-10 nm particles during summertime atmospheric nucleation events in urban Atlanta, *J. Geophys. Res*., *110*, D22S04, doi:10.1029/2005JD005918.

Stolzenburg, M. R., P. H. McMurry, H. Sakurai, J. N. Smith, R. L. Mauldin, III, F. L. Eisele, and C. F. Clement (2005), Growth rates of freshly nucleated atmospheric particles in Atlanta, *J. Geophys. Res.*, *110*, D22S05, doi:10.1029/2005JD005935.

Schlesinger, W. H., and A. E. Hartley (1992), A global budget for atmospheric NH_3, *Biogeochem.*, *15*, 191-211.

Shimshock, J. P., and R. G. DePena (1989), Below-cloud scavenging of tropospheric ammonia, *Tellus*, *41B*, 296-304.

Slusher, D. L., L. G. Huey, D. J. Tanner, F. M. Flocke, and J. M. Roberts (2004), A thermal dissociation–chemical ionization mass spectrometry (TD-CIMS) technique for the simultaneous measurement of peroxyacyl nitrates and dinitrogen pentoxide, *J. Geophys. Res.*, *109*, D19315, doi:10.1029/2004JD004670.

Smith, J. N., K. F. Moore, F. L. Eisele, D. Voisin, A. K. Ghimire, H. Sakurai, and P. H. McMurry (2005), Chemical composition of atmospheric nanoparticles during nucleation events in Atlanta, *J. Geophys. Res*. *110*, D22S03, doi:10.1029/2005JD005912.

Solomon, P. A., et al. (2003), Overview of the 1999 Atlanta Supersite Project, *J. Geophys. Res.*, *108*(D7), 8413, doi:10.1029/2001JD001458.

Weber, R. J., P. H. McMurry, L. Mauldin, D. J. Tanner, F. L. Eisele, F. J. Brechtel, S. M. Kreidenweis, G. L. Kok, R. D. Schillawski, and D. Baumgardner (1998), A study of new particle formation and growth involving biogenic and trace gas species measured during ACE 1, *J. Geophys. Res.*, *103*(D13), 16,385–16,396.

Weber, R. J., D. Orsini, Y. Duan, Y.-N. Lee, P. Klotz, and F. Brechtel (2001), A particle-into-liquid collector for rapid measurement of aerosol bulk chemical composition, *Aerosol Sci. Technol.*, *35*, 718-727.

Weber, R.J., D. Orsini, Y. Duan, K. Baumann, C.S. Kiang, W. Chameides, Y.L. Lee, F. Brechtel, P. Klotz, P. Jongejan, H.t. Brink, J. Slanina, P. Dasgukpta, S. Hering, M. Stlozenburg, E. Edgerton, B. Hartsell, P. Solomon, and R. Tanner (2003), Intercomparison of near real-time monitors of PM2.5 nitrate and sulfate at the EPA Atlanta Supersite, *J. Geophys. Res.*, 108 (D7), 10.1029/2001JD001220.

Wells, M., T. W. Choularton, and K. N. Bower (1998), A modelling study of the interaction of ammonia with cloud, *Atmospheric Environment*, *32*, 359-363, doi:10.1016/S1352-2310(97)00199-4.

Wexler, A. S., and J. H. Seinfeld (1991), 2nd-generation inorganic aerosol model, *Atmos. Environ. Part A*, *25*, 2731-2748.

Wexler, A. S., and J. H. Seinfeld (1992), Analysis of aerosol ammonium nitrate: departures from equilibrium during SCAQS, *Atmos. Environ. Part A*, *26*, 579-591.

Zhang, J., W. L. Chameides, R. Weber, G. Cass, D. Orsini, E. S. Edergton, P. Jongejan, and J. Salina (2002), An evaluation of the thermodynamic equilibrium assumption for fine particulate composition: Nitrate and ammonium during the 1999 Atlanta Supersite Experiment, *J. Geophys. Res.*, *107*, 8414, doi:10.1029/2001JD001592, [printed *108*(D7), 2003].

Figure Captions

Figure 1. NOAA-CSD Instrument Schematic

Figure 2. Mass spectrum from NOAA-CSD instrument taken on 27 August 2002. The primary reagent ion clusters, $(EtOH)H^+$ (47 amu), $(EtOH)_2H^+$ (93 amu), $(EtOH)_3H^+$ (139 amu), and the primary product ions, NH_4^+ (18 amu) and $(EtOH)NH_4^+$ (64 amu) are labeled.

Figure 3. GT Instrument Schematic

Figure 4. Percent of signal after removal of a 2 ppbv standard addition calibration as a function of time for the NOAA-CSD (blue) and GT (red) instruments. The triple exponential fit for each is shown in black. The 1/e time for both instruments is less than 10 s and the $1/e^2$ time is less than 1 min.

Figure 5. One-minute NOAA-CSD observations plotted against 1-min GT observations.

Figure 6. Time series of the NOAA-CSD (blue) and GT (red) NH_3 observations plotted from 19 August to 29 August.

Figure 7. Plotted are the hourly averages (solid line) and hourly medians (bar) for NH_3, CO, and NOy versus Eastern Standard Time (EST). The horizontal bars represent the 25^{th} and 75^{th} percentiles of the hourly averages.

Figure 8. Hourly averages (solid line) and hourly medians (bar) for the NH_3 observations (top panel) and CMAQ predictions (bottom panel). The horizontal bars represent the 25^{th} and 75^{th} percentiles for each hour.

Figure 9. Same as Figure 8, for NH_4^+.

Figure 10. Same as Figure 8, for NO_3^-.

Figure 11. Same as Figure 8, for SO_4^{2-}.

Figure 12. Model predictions constrained by total ammonia ($NH_3 + NH_4^+$) plotted against the GT NH_3 observations. Unweighted linear regression analysis yields a slope of 1.25 with an intercept of 0.012 $\mu g\ m^{-3}$ and an r^2 of 0.75.

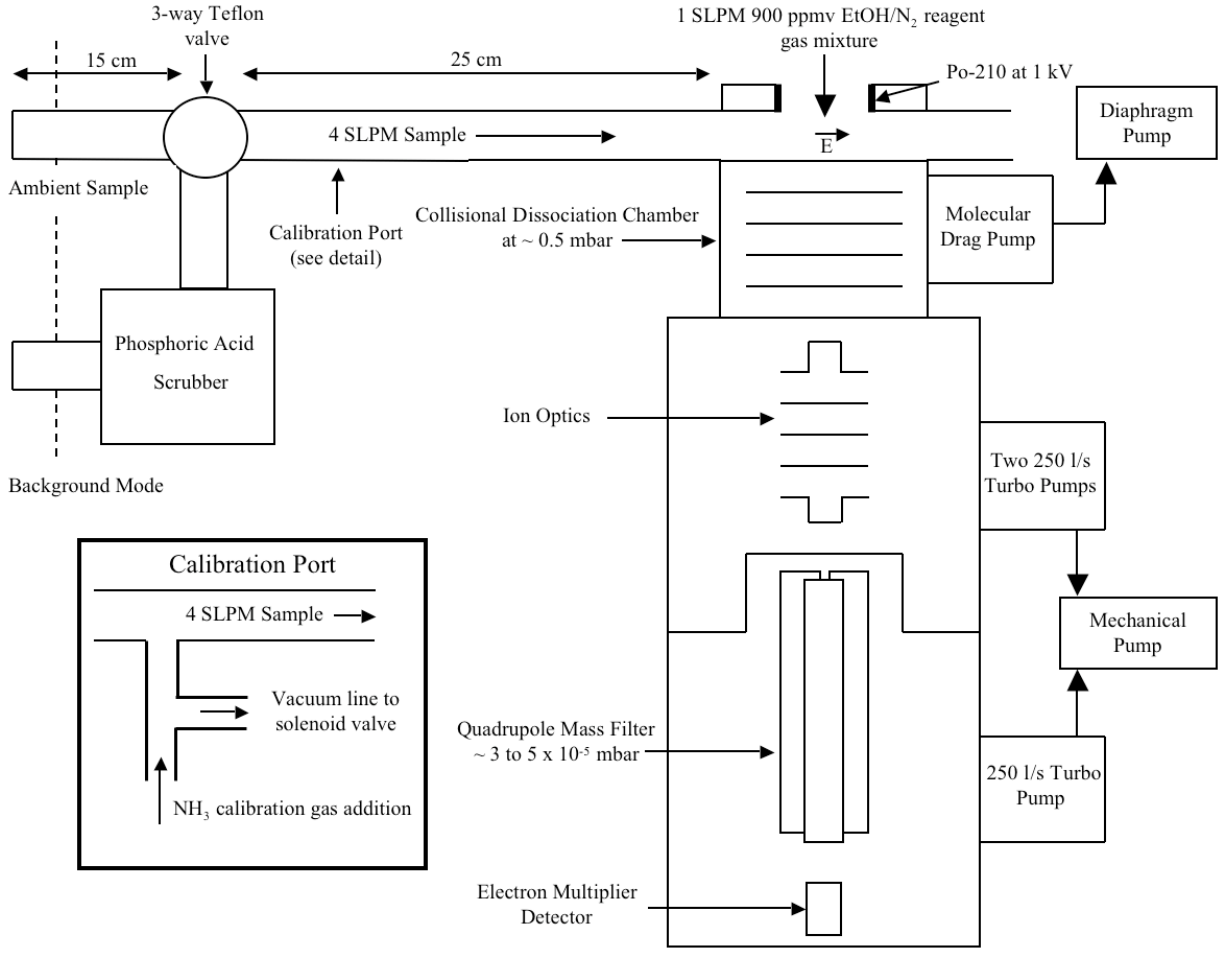

Figure 1. NOAA-CSD Instrument Schematic

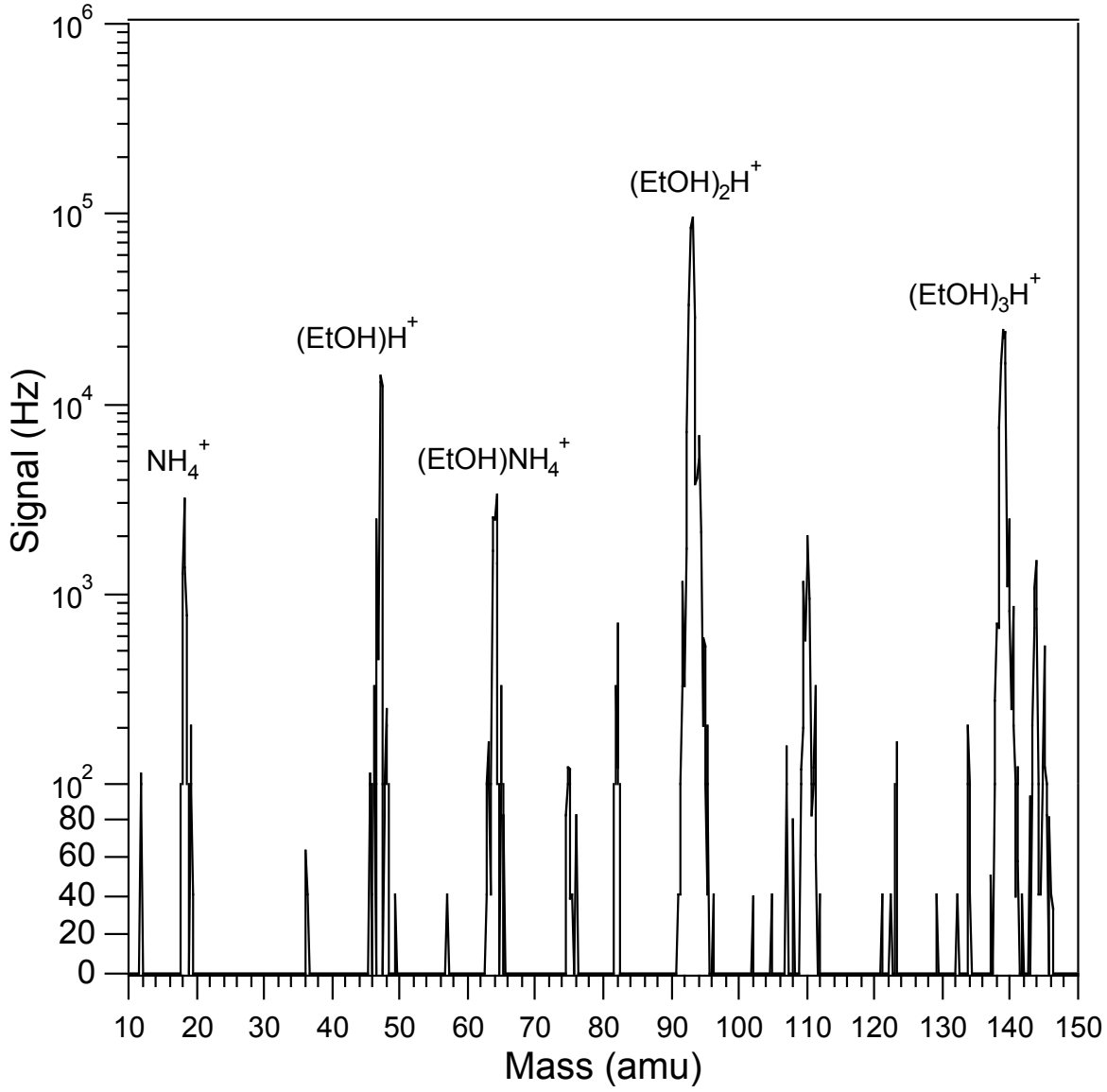

Figure 2. Mass spectrum from NOAA-CSD instrument taken on 27 August 2002. The primary reagent ion clusters, $(EtOH)H^+$ (47 amu), $(EtOH)_2H^+$ (93 amu), $(EtOH)_3H^+$ (139 amu), and the primary product ions, NH_4^+ (18 amu) and $(EtOH)NH_4^+$ (64 amu) are labeled.

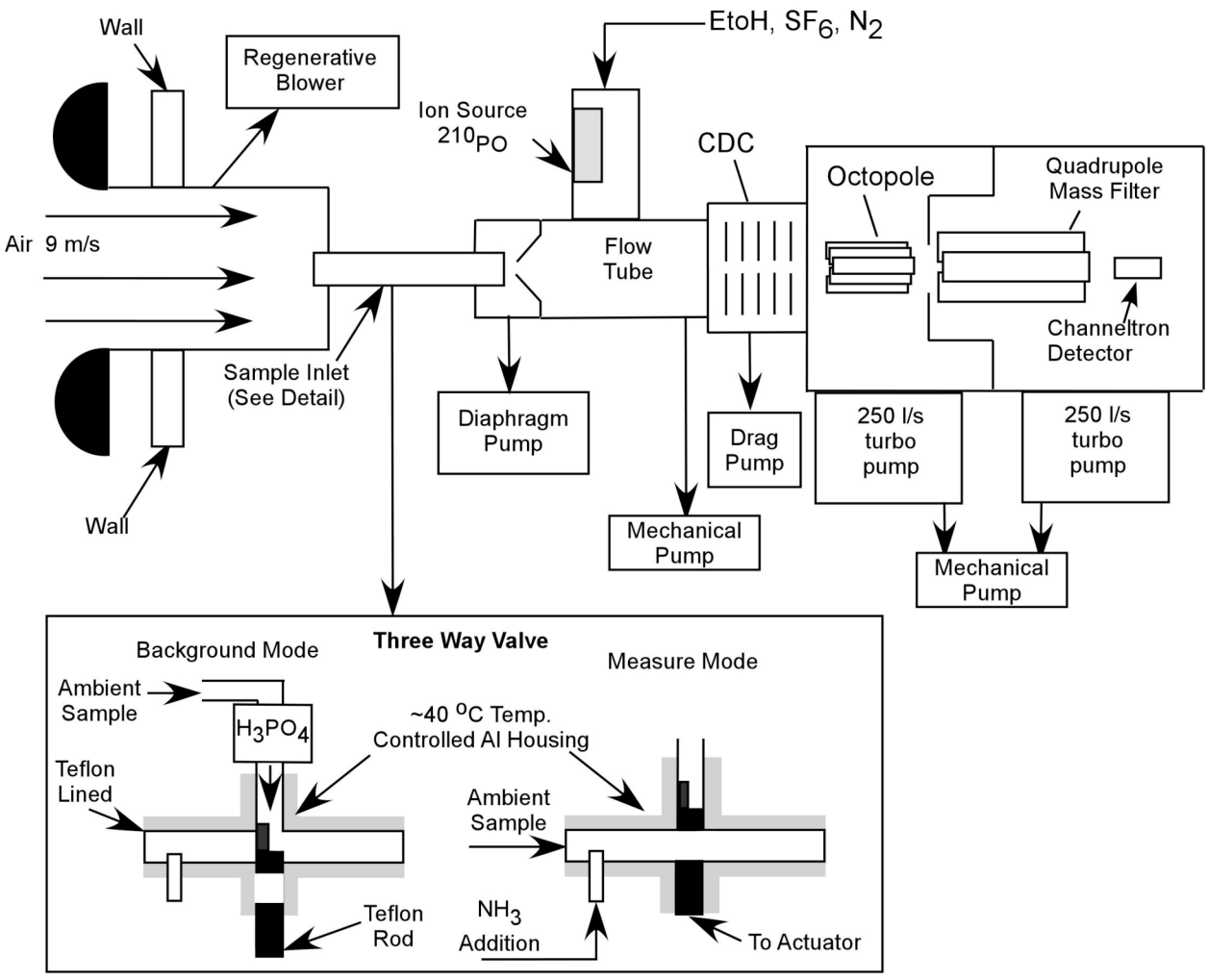

Figure 3. GT Instrument Schematic

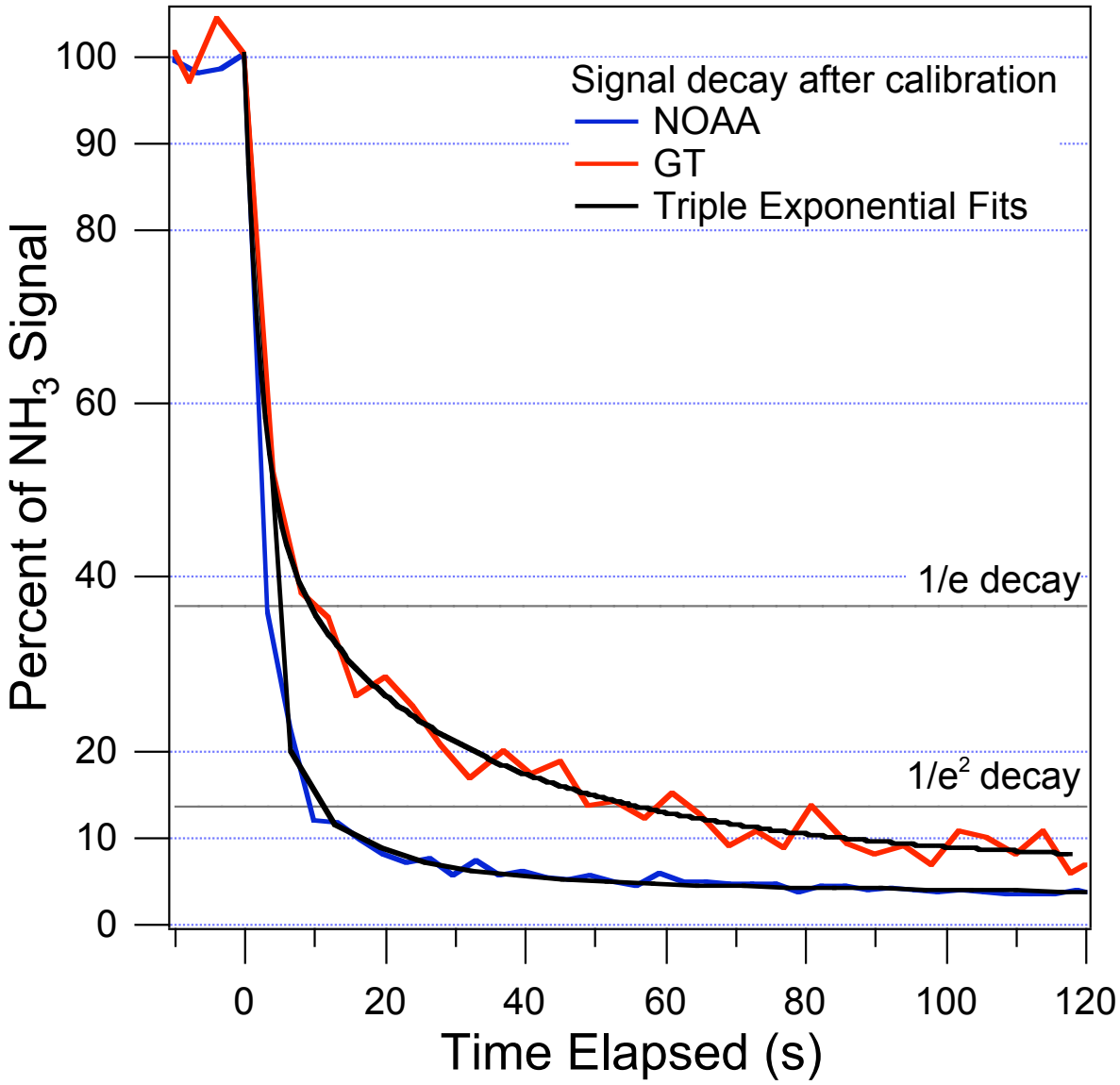

Figure 4. Percent of signal after removal of a 2 ppbv standard addition calibration as a function of time for the NOAA-CSD (blue) and GT (red) instruments. The triple exponential fit for each is shown in black. The 1/e time for both instruments is less than 10 s and the $1/e^2$ time is less than 1 min.

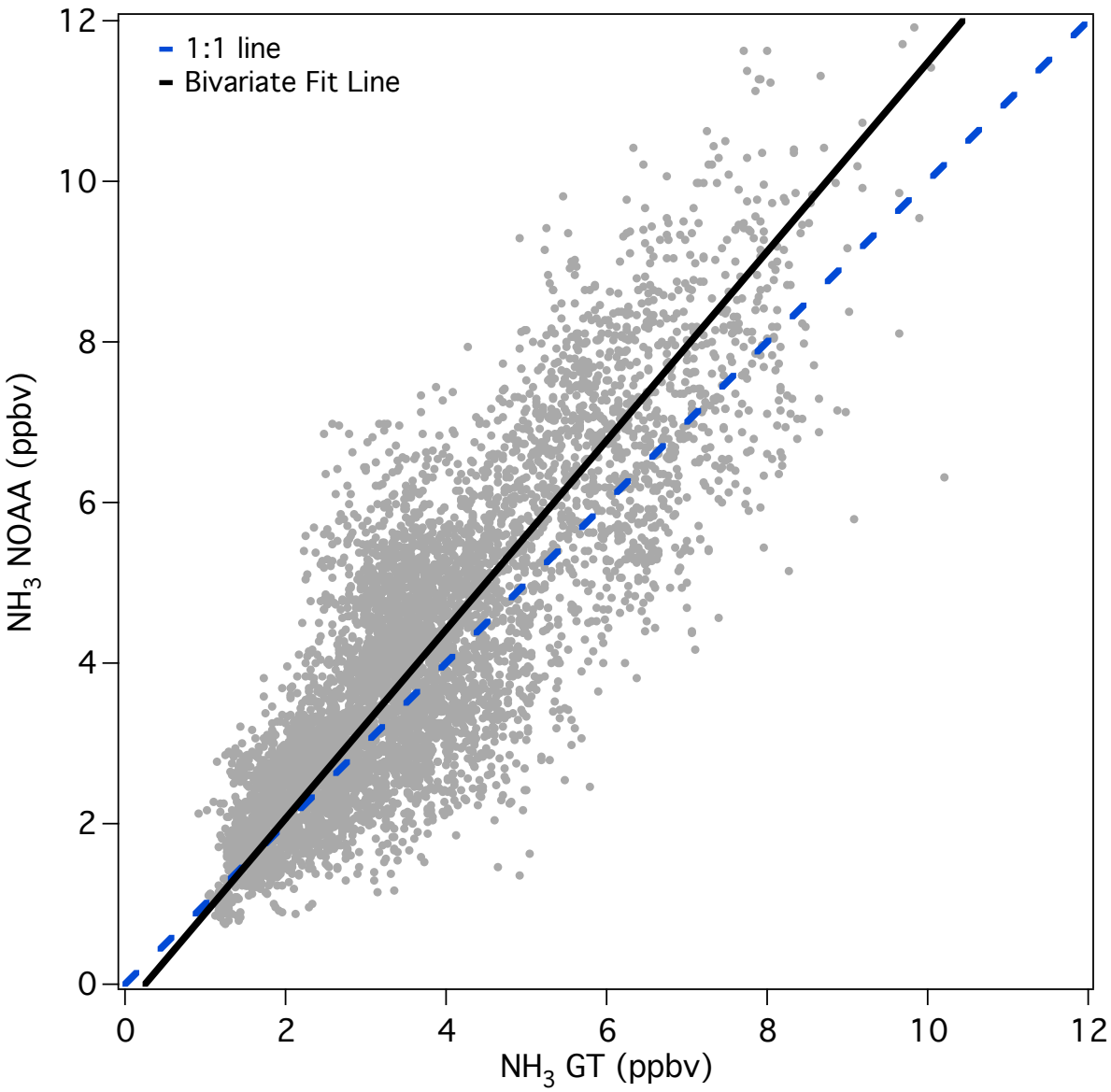

Figure 5. One-minute NOAA-CSD observations plotted against 1-min GT observations.

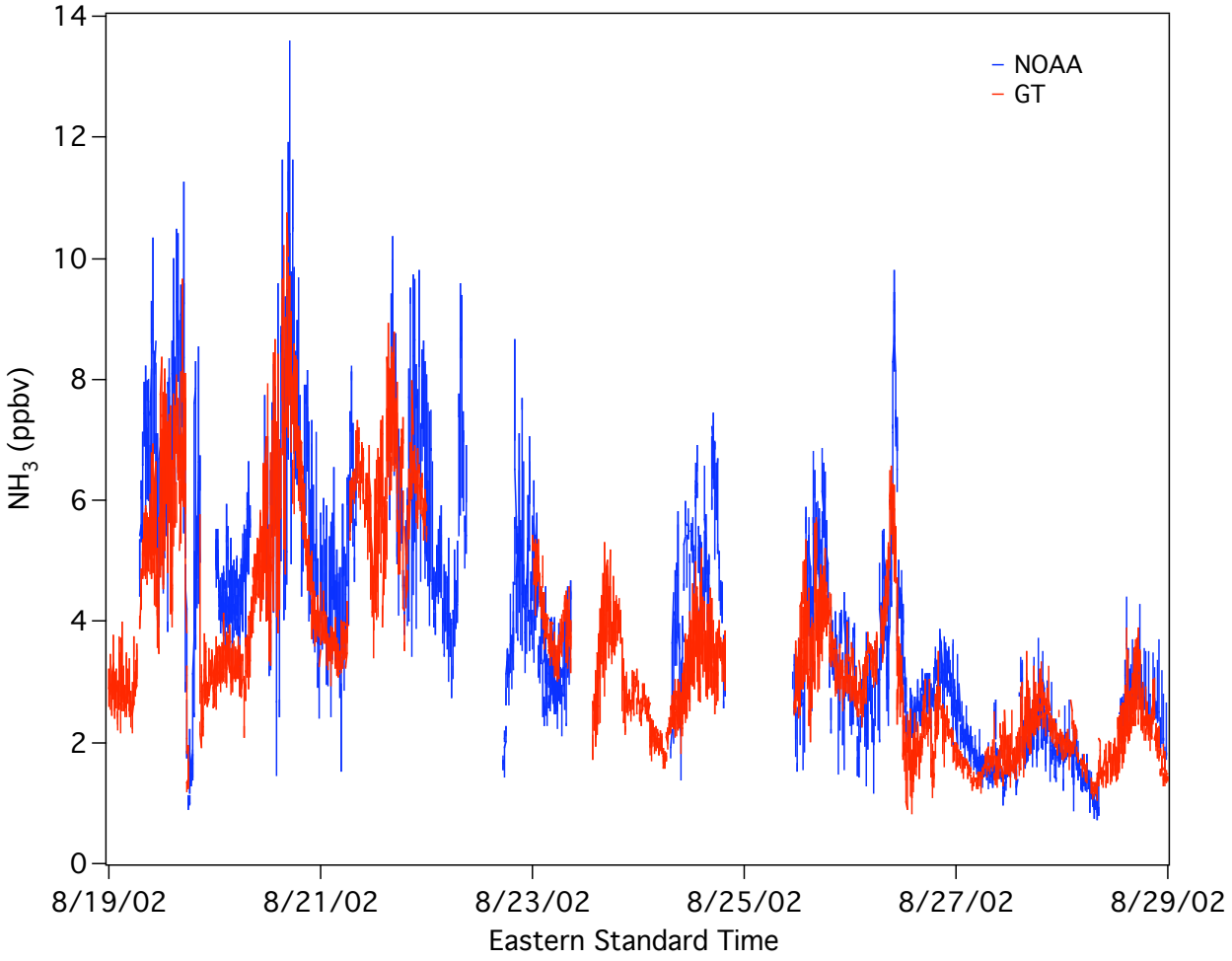

Figure 6. Time series of the NOAA-CSD (blue) and GT (red) NH_3 observations plotted from 19 August 2002 to 29 August 2002.

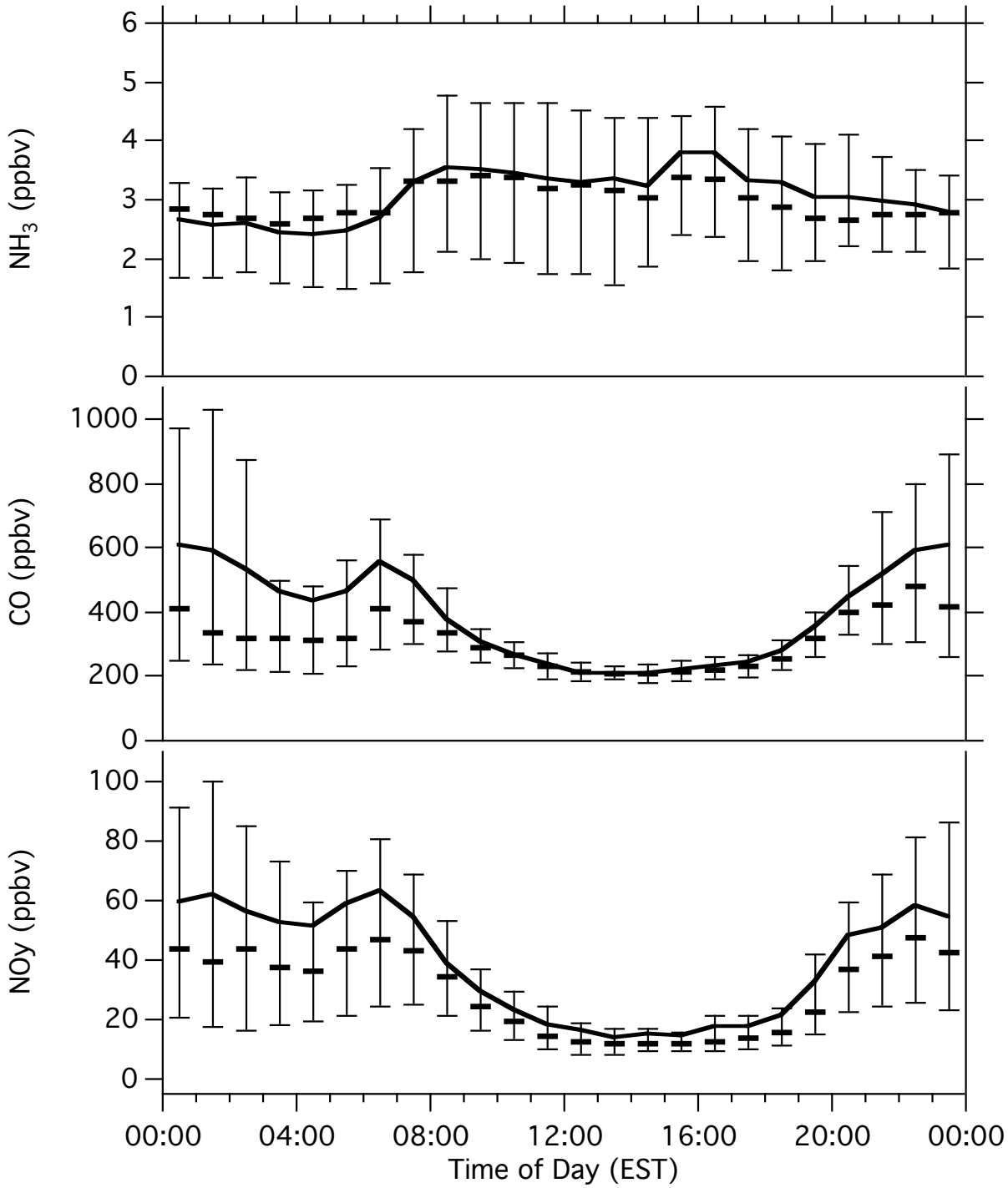

Figure 7. Plotted are the hourly averages (solid line) and hourly medians (bar) for NH_3, CO, and NOy versus Eastern Standard Time (EST). The horizontal bars represent the 25^{th} and 75^{th} percentiles of the hourly averages.

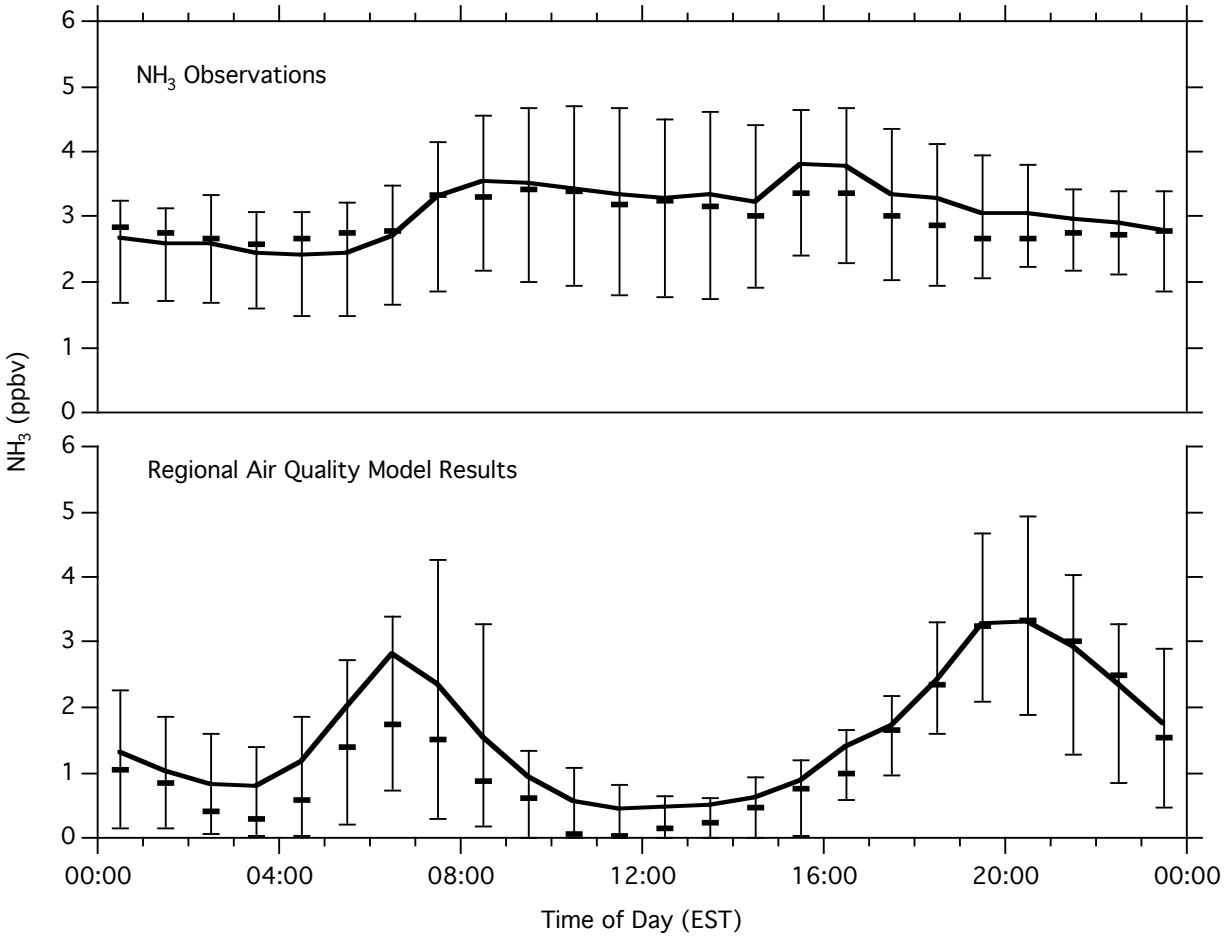

Figure 8. Hourly averages (solid line) and hourly medians (bar) for the NH_3 observations (top panel) and CMAQ predictions (bottom panel). The horizontal bars represent the 25th and 75th percentiles for each hour.

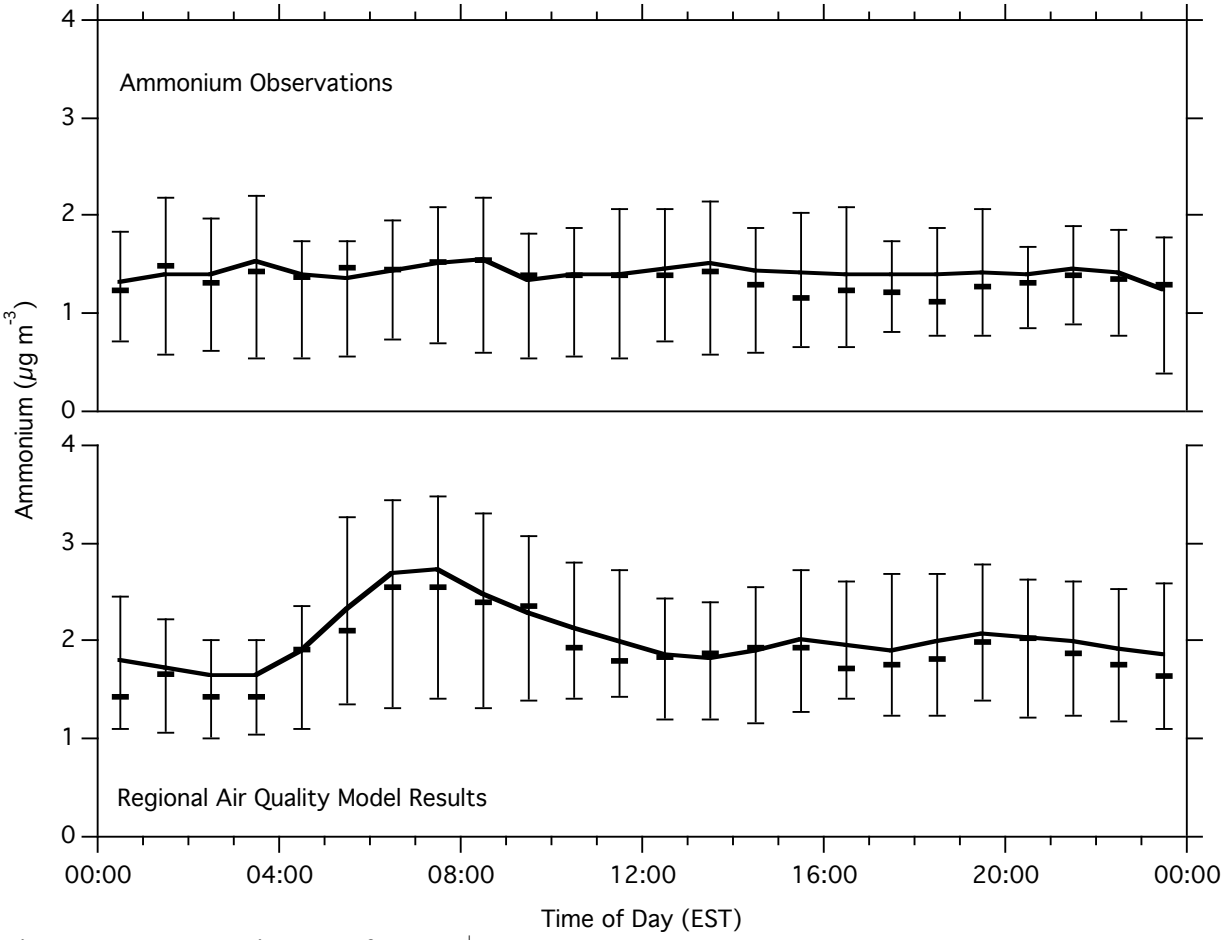

Figure 9. Same as Figure 8, for NH_4^+.

1

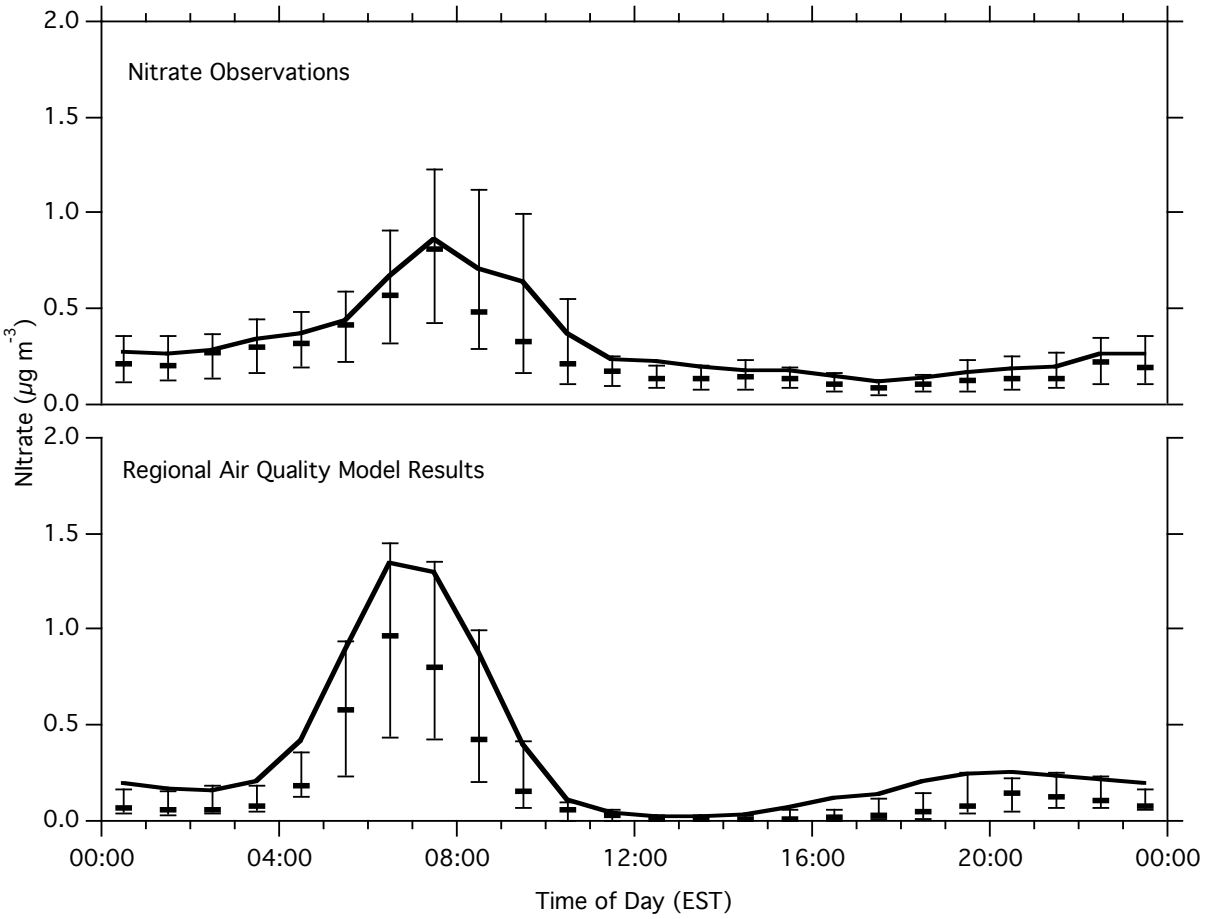

2

3 Figure 10. Same as Figure 8, for NO_3^-.

4

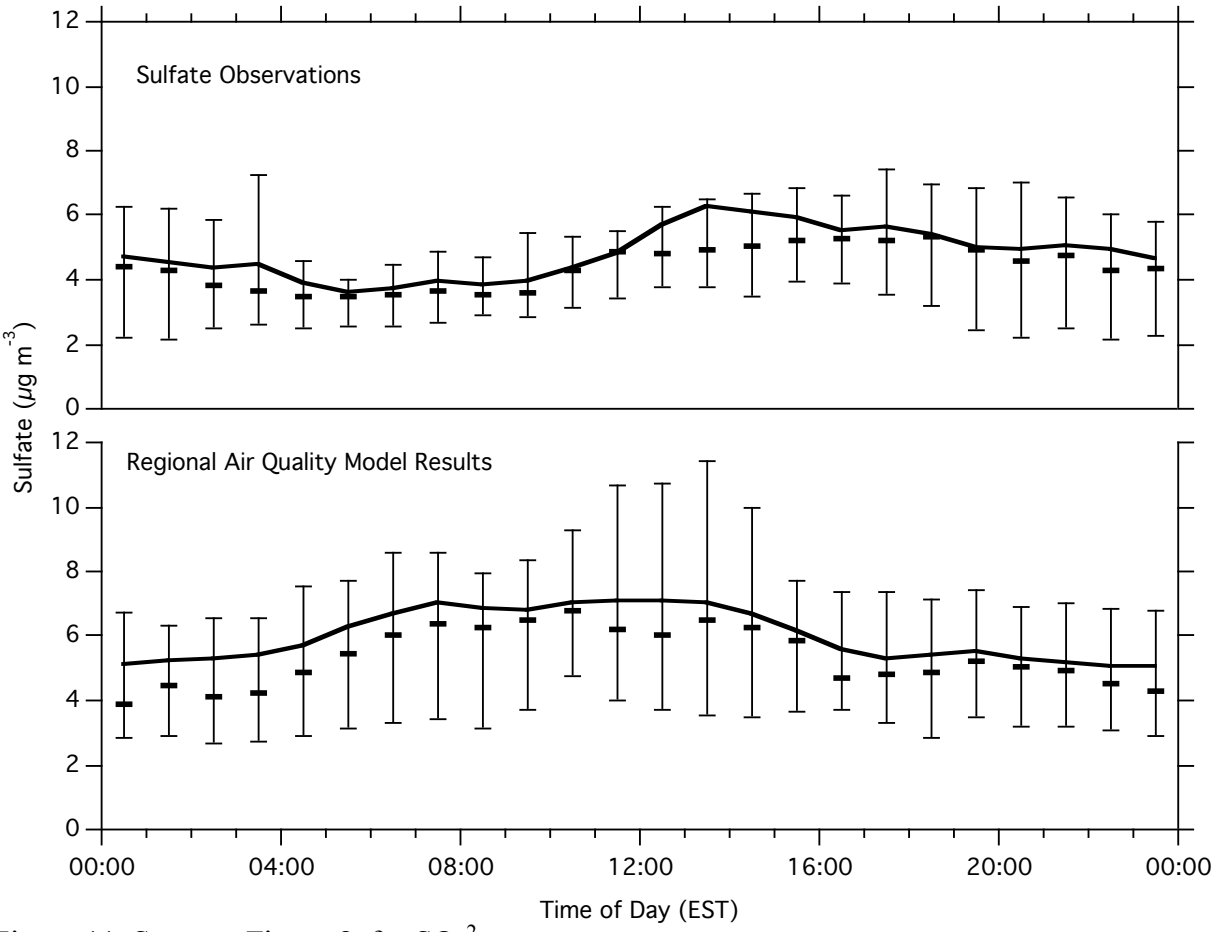

Figure 11. Same as Figure 8, for SO_4^{2-}.

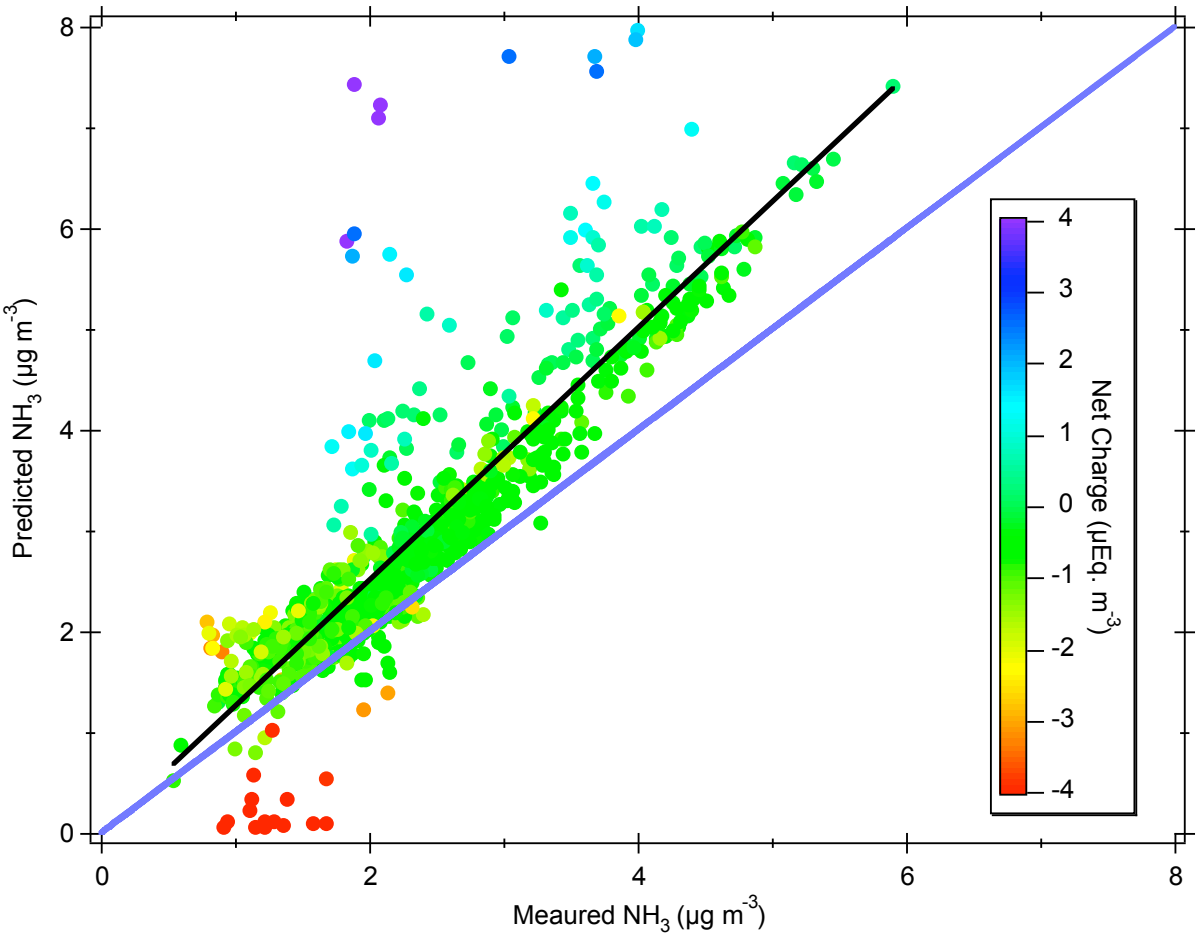

Figure 12. Model predictions constrained by total ammonia ($NH_3 + NH_4^+$) plotted against the GT NH_3 observations. Unweighted linear regression analysis yields a slope of 1.25 with an intercept of 0.012 µg m^{-3} and an r^2 of 0.75.